

Optimal Phase Lock at Femtowatt Power Levels for Coherent Optical Deep-Space Transponder

G. John Dick,* Meirong Tu,* Dmitry Strelakov,* Kevin Birnbaum,* and Nan Yu*

We report on results of the first tests of an optical phase-lock loop (PLL) with the capability to recover an optical carrier at powers below one picowatt (pW), as required for a deep-space coherent optical transponder. In such an application, a limiting phase variation is due to instability in the (optical) frequency standard that provides a phase reference at the return of the transponded signal, possibly many minutes later. We present results showing a PLL phase-slip rate *below* one cycle slip per second at powers as low as 40 femtowatts (fW). This phase-slip rate corresponds to a frequency stability of $\delta f/f \approx 1 \times 10^{-14} / \sqrt{\tau}$, a value better than any frequency standard available today for measuring times equal to a typical two-way delay between Earth and Mars, and the < 100 fW required power allows application at Mars' farthest distance from Earth with a reasonable transmitter power level ($P < 5$ W). Parameters for a second-order PLL were optimized for the laser-noise and shot-noise levels by use of simulation software. Good agreement was obtained between laboratory measurements and the simulation results. We also report on measurements of the phase noise of the fiber lasers used for the test, analysis of the limitations on PLL performance at low optical power implied by this laser noise level, the results of demonstrations of Doppler signals at fW power levels, and transponder architectures designed to take advantage of this capability to achieve micron-level ranging accuracy with very short measuring times.

I. Introduction

We report here on the results of experiments, calculations, and demonstrations designed to establish the feasibility of a deep-space coherent optical transponder based on an optical phase-locked loop (PLL) scheme. To this end, we have modeled, developed, and tested optical PLLs that operate at picowatt (pW) and femtowatt (fW) power levels. The excellent performance obtained — that is, low cycle-slip rates at very low optical power levels — make the PLL-based optical transponder an attractive prospect for deep space spacecraft. Implemented in a Mars mission, an optical transponder could increase both ranging and Doppler accuracies by more than 10 times compared to present technology, while reducing acquisition time by ≈ 100 times.

*Communication Architectures and Research Section.

The research described in this publication was carried out by the Jet Propulsion Laboratory, California Institute of Technology, under a contract with the National Aeronautics and Space Administration. © 2008 California Institute of Technology. Government sponsorship acknowledged.

To our knowledge, the results presented here represent the first measurements and demonstrations of optical phase lock at sub-pW power levels. We report here the characterization of an optical PLL at powers as low as 40 fW with low cycle-slip rates (1 per second). This was achieved by the use of modern fiber lasers with a very narrow linewidth, and by use of simulation software that we developed to optimize PLL parameters for low cycle-slip rates in the presence of both laser noise and substantial photon shot noise due to the very low powers involved.

While calculations were previously available for the minimization of PLL cycle slips in the presence of shot noise [1], previous work did not include any equivalent to the strong laser local oscillator (LO) noise present in a laser PLL. In fact, the previous work always predicted poorer performance with the addition of a second-order loop, while the flicker-frequency noise in our lasers requires such a second-order loop for stable operation. Thus, a new calculation methodology was required: We chose a sequential time simulation methodology for its ability to accurately account for virtually any noise and phase-detector models.

We also report on characterization of the phase noise and (inferred) bandwidth of the two fiber lasers, characterization of detected shot-noise levels at low power, and relative intensity noise (RIN) for the lasers, and we discuss the implications of these characteristics in relationship to optical PLL design at very low power levels. An experimental method was developed that allows cycle slips to be directly observed, and to be characterized in terms of the spectrum of a measured signal. A comparison of the achieved PLL performance and results of the simulation shows excellent agreement.

Several possible optical transponder architectures are presented together with their associated spectra, including a pseudorandom range code (PRRC) model, a second model with added 100-MHz subcarrier that shows improved ranging performance and reduced detection bandwidth requirements, and a third model with an added 10-GHz subcarrier for ultrahigh ranging performance. Design considerations are discussed, including performance limitations due to the required optical frequency standard in the “base” unit, and problems due to the RIN spectrum and the frequency and bandwidth available from a required shot-noise limited optical detector.

Finally, the results of two free-space demonstration experiments are presented. These experiments include a variable-length optical path that is implemented by means of a moveable corner-cube reflector supported by an “air track.” In the first of these experiments, optical phase lock to the time-varying signal was demonstrated at the 1-pW level with relatively high acceleration of the reflector ($\approx 0.3 g$, achieved by means of attached springs) that simulated typical spacecraft Doppler rates. For the second experiment, a configuration was developed where a PLL locked to a very low power optical signal from the moveable mirror (150 fW) was compared with a high-power signal, showing an RMS variation for 1-s frequency measurements of ≈ 0.2 Hz. This corresponds to a short-term frequency stability of 1×10^{-15} at 1 s measuring time, well matching the performance of the very best optical frequency sources that have been demonstrated to date.

II. Background

Microwave transponders on spacecraft, together with ultrastable clocks on the ground, presently enable the ultra-accurate ranging capability required by deep-space navigation and radio science. Over the past decades, microwave frequencies and ranging performance have both steadily increased, culminating in the 8.4-GHz/32-GHz (X-band/Ka-band) transponders used in the Cassini mission for navigation, ring and atmospheric occultation experiments, and a search for gravitational waves. An obvious advantage of higher frequency is the reduction of diffractive losses on both Earth-based and spacecraft-based antennas due to the shorter wavelength. Just as important, however, is a markedly increased immunity of higher-frequency electromagnetic radiation to effects of the (ionized and unstable) solar wind. The culmination of this progression would be an “optical transponder” using light at optical or infrared wavelengths to provide a dramatic improvement in ranging performance compared to any microwave transponder [2].

As an example application, consider a spacecraft for a Mars mission, where the farthest distance from Earth is approximately 2.5 AU. For such a mission, and for base and spacecraft antennas of 1-m and 10-cm diameters, respectively, a requirement of 1 pW received optical power requires a 55-W optical source at each end. Clearly, a ≈ 5 -W transmitter is a much more attractive prospect for the spacecraft transmitter, requiring operation with received powers of 100 fW or below. We report here experimental results for optical PLL operation that show low cycle-slip rates at optical power levels as low as 40 fW.

Advantages promised by an optical transponder over the present technology include both improved absolute performance, that is, ranging and Doppler (frequency) accuracy; and a short measuring time required to establish that performance. The advantage for Doppler measurements is particularly great because of the extremely short wavelength of the optical carrier — thus, for any given velocity, the frequency offset is much greater. Similarities to the microwave approach include use of the combination of pseudorandom code together with single-tone subcarriers to establish the absolute range, and the use of the carrier frequency (microwave or optical) for Doppler measurements.

III. Laser Phase Noise Characterization

In the presence of only shot noise, cycle slips in a PLL can be reduced to any desired level by reducing the loop bandwidth [1]. However, with a free-running laser LO, optical PLL performance at the lowest possible optical power levels is always limited by the presence of low-frequency laser noise.¹ This noise is typically white-frequency or flicker-frequency noise, which, with $1/f^2$ or $1/f^3$ spectra (respectively) at low frequency offsets, eventually dominates any shot noise value as the frequency is lowered. What this means for phase locking is that narrowing of the loop bandwidth fails at some point to improve the cycle-slip rate, and furthermore, that the rate will in fact increase if the bandwidth is further narrowed. Thus, a detailed knowledge of the laser phase noise is necessary in order to predict and optimize low-power PLL performance with any real laser.

¹ The “spectra” described here are measures of $S_{\phi}(f)$, with units of rad^2/Hz , and which for additive shot noise is numerically equivalent to the inverse of the RF or optical signal to noise, described as $\text{dBc}/(\text{Hz})$.

The general test setup for phase-noise measurements is shown in Figure 1. All measurements were obtained in a closed-loop setup for stability and reproducibility. The phase-locked loop is a combination of RF and optical circuitry. After detection of a heterodyne of the weak signal with an added LO signal at about 100 MHz, the detected signal is phase locked to a synthesized signal by means of PLL circuitry that combines a second-order loop with variable parameters that is used in a “fast” loop that controls the frequency of an approximately 100-MHz VCO driving an acousto-optic modulator (AOM), and whose action is complemented by a very slow loop controlling the piezo frequency control incorporated into the laser.

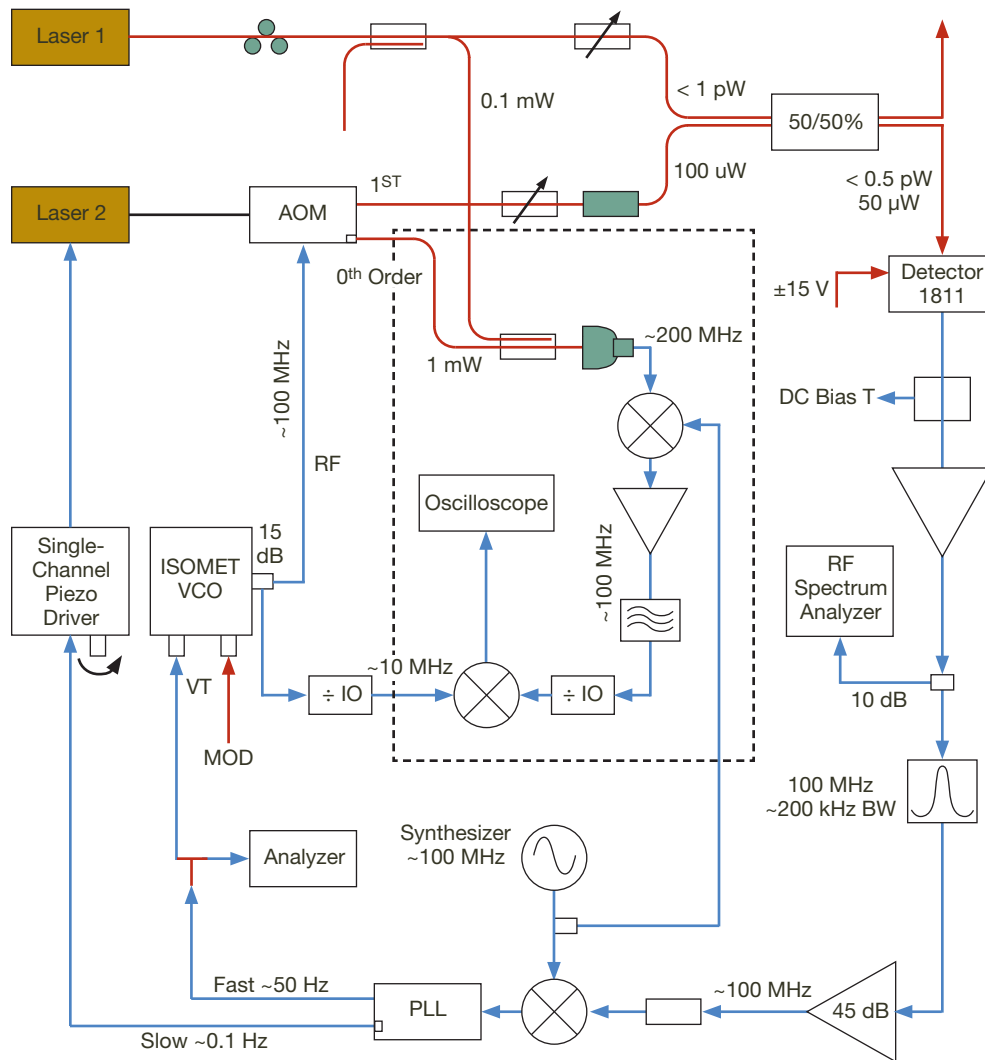
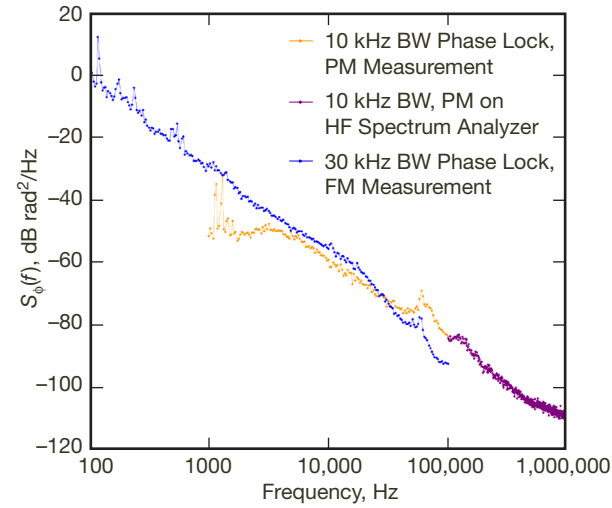
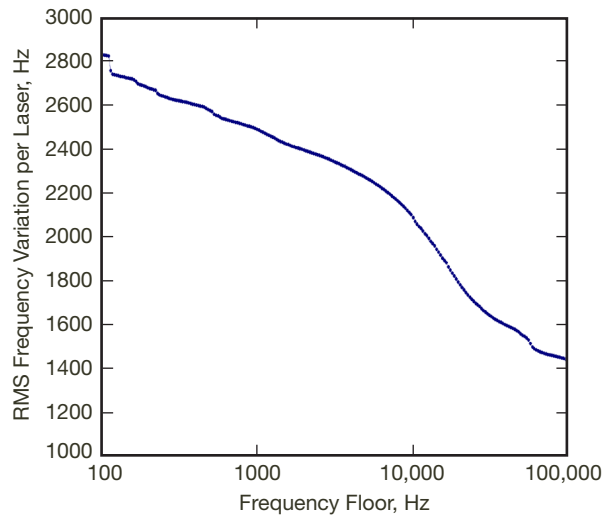


Figure 1. Block diagram of the general measurement test setup. Phase-noise data are typically obtained from the “Analyzer” signal, while components in the dashed box are added in order to measure cycle slips and their associated phase noise.

A summary of our laser phase noise characterization results is shown in Figure 2. Figure 2(a) shows two separate curves that combine to show a spectral density of phase fluctuations $S_{\phi}(f) \propto 1/f^3$ over a wide frequency range: the lower frequency results were measured as frequency fluctuations in a closed-loop setup with a relatively high-loop bandwidth while the higher-frequency curves were measured as phase fluctuations with a narrow-loop bandwidth — effectively an open-loop setup. Examination of the curves shows deviation downward in both cases for frequencies above, or below, the loop bandwidth, respectively. A straight-line value $S_{\phi} = 60 \text{ dB/Hz} \times (1 \text{ Hz}/f)^3$ derived from this plot was used in our PLL



(a)



(b)

Figure 2(a). Measured phase noise for two Koheras distributed-feedback (DFB) lasers. Measurements at lower frequencies (blue curve) were made in a closed-loop configuration, derived from frequency noise measurements via the frequency error feedback into a voltage-controlled oscillator (VCO) in the phase-locked loop.

(b). Laser bandwidth for each Koheras laser, calculated from curve (a) for various values of the measuring time (or equivalently, frequency floor). Values are somewhat higher than the $\approx 1\text{-kHz}$ bandwidth estimated by the manufacturer.

simulations as the two-laser phase noise. As will be shown later, simulations based on this model gave good agreement with experimental phase-slip measurements.

Figure 2(b) shows the single-laser bandwidth derived from part (a) for varying values of a lower cutoff or “floor” frequency. The values are somewhat larger than the specifications for our fiber lasers,² which indicate a < 1-kHz optical bandwidth for a measuring time of 120 μ s.

Figure 3 shows a sequence of phase-noise measurements with differing values of optical power. The measurements were made using our “usual” frequency fluctuation measurement configuration, and the data show the effects of a high-frequency cutoff corresponding to the loop bandwidth. From this data set and comparison to a curve fitted to the 75-pW data below the cutoff by addition of a constant value to the “higher power lock” curve, we conclude that the measured signal to noise is 6.5 dB poorer than the shot-noise limit, calculated on the basis of the measured input optical power to the detector. This loss is primarily due to detector inefficiency and optical mismatch in the detector between the 50- μ W LO (heterodyne) signal and the weak 75-pW signal.

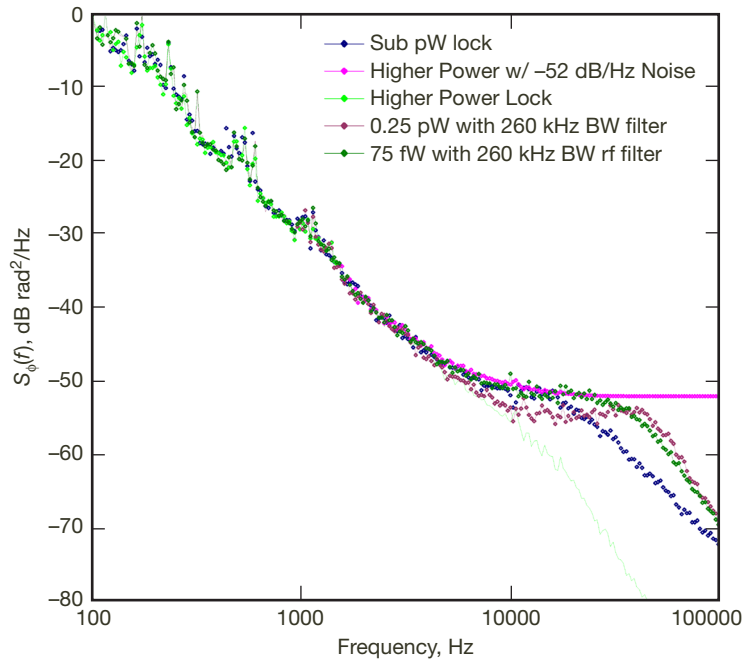


Figure 3. Measured phase noise for two Koheras fiber lasers at very low power showing the onset of shot noise. The $-52 \text{ dB rad}^2/\text{Hz}$ apparent asymptote for the 75-pW curve is just 6.5 dB above the theoretical value of $-58.5 \text{ dB rad}^2/\text{Hz}$ for that power level. Typical values obtained were 4 to 6 dB above the theoretical shot-noise value.

² See <http://www.koheras.com>.

IV. Laser Relative Intensity Noise (RIN)

Our choice of an approximately 100-MHz heterodyne frequency for the optical PLL setups is largely driven by RIN (amplitude noise) in our lasers. Figure 4 shows a plot of the measured RIN spectrum. The figure shows that the RIN is substantially sensitive to laser operation parameters, so that, e.g., the 50- μ W LO signal will have more RIN if it is derived from a 4-mW laser output than a similar signal derived from a higher laser output of 6 mW. We typically operate the lasers at an output level of 17 mW for best noise and stability performance.

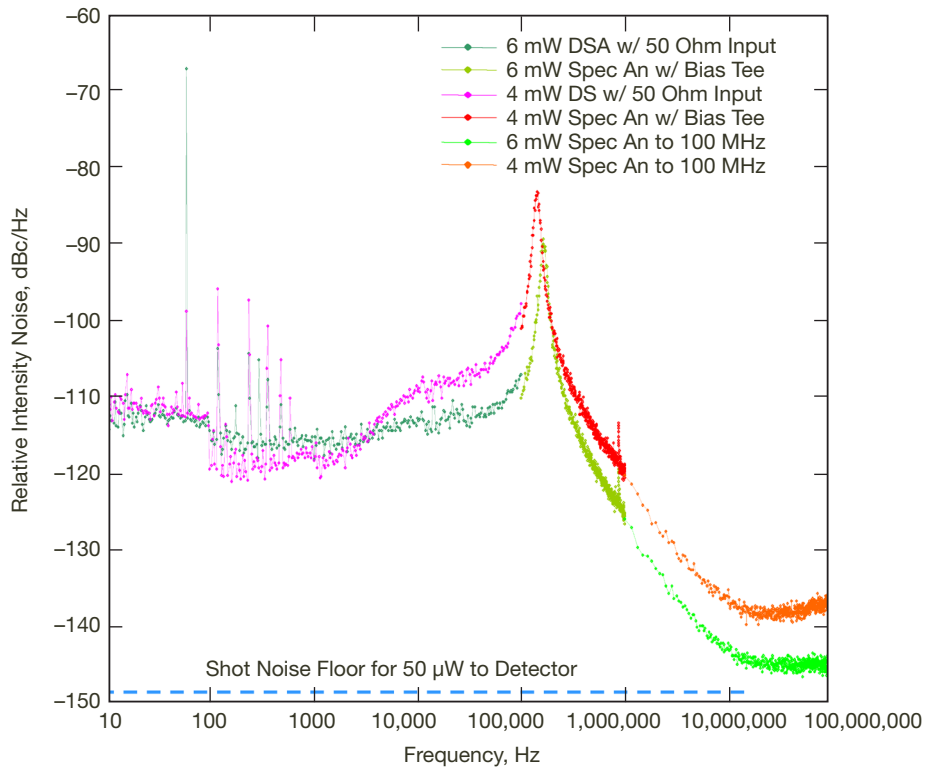


Figure 4. Relative intensity noise (RIN) for one laser. Notice that the peak near 100 kHz shifts with laser power. The approach to shot-noise-limited performance between 20 MHz and 100 MHz points to this region for offset (heterodyne) and subcarrier frequencies. For this reason, all phase-lock experiments were conducted with an injected signal that was offset by 50 MHz to 100 MHz.

While it is possible to reject RIN in the injected LO (heterodyne) signal to a substantial degree by the use of balanced and complementary phase detectors, achieving shot-noise-limited performance is made easier by the use of a single high-quality optical detector. Amplitude noise is also nominally rejected by our RF mixer phase detector, but this only by 20 dB or so. As can be seen from Figure 4, RIN can be reduced to nearly the shot-noise value with higher power outputs from the fiber laser, and for frequencies above about 50 MHz.

V. Loop Simulation to Optimize PLL Performance

We have developed software that simulates PLL operation in the face of the various noise processes present in our system. PLL performance limitations due to photon (shot) noise has been previously studied by Viterbi [1] for a first-order PLL. Somewhat poorer results for a second-order loop have also been reported. Because the fiber lasers used³ show flicker-frequency noise with a $1/f^3$ power spectrum over much of the frequency range, a second-order loop is required, and the optimization of such a system for the lowest possible level of cycle slips has not been previously reported. We verified the operation of our software by recovering the Viterbi result, and also found good agreement with Laser Interferometer Space Antenna (LISA) project calculations for their Non-Planar Ring Oscillator (NPRO) lasers (which typically show “white-frequency” noise with a $1/f^2$ power spectrum.⁴ A typical software run involved generating 1 to 4 million random phase variations with the various noise models required. The results of one of these runs is shown in Figure 5. This particular run shows the very highest white phase noise level (-51 dB rad²/Hz) that we could achieve (withstand) by variation of the first- and second-order loop gains; all the while keeping the cycle-slip rate below 1 per second.

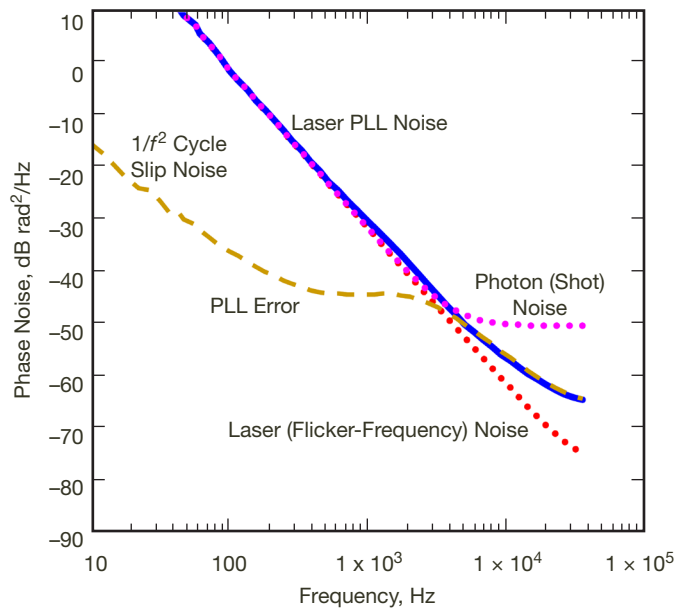


Figure 5. Simulation calculation of PLL performance optimized for the highest possible shot-noise level (-51 dB/Hz) that allows a cycle-slip rate of 1 cycle slip per second as shown by a $\approx 2/f^2$ (/Hz) noise contribution to the PLL error signal. The $+60$ dB/ f^3 flicker-frequency noise imposed on the PLL simulation well matches the (two-laser) measured noise values.

In addition to the “white” and “flicker frequency” noise processes shown in Figure 5, a small amount of “random walk frequency” noise with a $1/f^4$ spectrum was also added, in an amount too small to be seen on the graph; without such an added noise the simulated PLL would never actually “lose lock,” behavior that is typically (and often) seen in the laboratory.

³ See <http://www.koheras.com>.

⁴ Robert Spero, personal communication, Jet Propulsion Laboratory, Pasadena, California.

It was not found necessary to identify “cycle-slip” events in the software, since their effect is shown with a particular signature in the phase noise of the phase-locked oscillator. Thus, we can quantify the cycle-slip rate for Figure 5 as rate = 1 (per second) from the level of “random walk of phase” (identical to “white frequency”) noise, which has a characteristic $1/f^2$ frequency dependence. The dependence is given by $S_{\phi}(f) = 2/f^2 \times \text{rate} (/Hz)$,⁵ corresponding to +3 dB $-20 \times \log(f)/(Hz)$, as plotted in the figure.

The simulation software was able to model the performance of the PLL with various models for the phase-detection element in addition to the sinusoidal response shown by the RF mixers that were actually used. Typically, 1 or 2 dB improvement was possible with the use of phase-detector models that show a wider phase range for “linear” phase response than is given by the sinusoidal model, and a small improvement was also found for algorithms that tend to ignore the amplitude of the signal (which RF mixers do not). However, the small improvements found did not justify implementing a more complex (and possibly noisier) phase-detection system.

For any given shot-noise level, the simulation allowed the first- and second-order loop parameters to be optimized so as to minimize the cycle-slip rate. Additionally, the highest possible shot-noise level for an optimized loop could be determined for any given cycle-slip rate. The results shown in Figure 5 have been optimized by adjustment of the loop parameters for a cycle-slip rate of 1.0 (per second), and indicate that this rate can be achieved with a shot noise level of -51 dB rad²/Hz; which, with a perfect (shot-noise-limited) optical detector and an ideal RF system, would correspond to a power level of 13 fW (at an optical wavelength of 1550 nm). Even though our systems show noise levels that are typically 4 to 6 dB higher than the ideal, on the basis of this simulation data it seems clearly possible to achieve phase lock with optical powers far below the ≈ 1.2 nW previously reported [3].

VI. Optical Phase Locking at Femtowatt Power Levels

Previous work in support of the ASTROD [3,4,5] and LISA⁶ [6] space missions have reported optical PLL operation at powers down to ≈ 1.2 nW and 75 nW, respectively. We have been able to achieve optical phase lock with actual optical power into the optical (heterodyne) detector of 40 fW, with no more than 1 cycle slip per second. Figure 1 shows a block diagram of the circuitry used to make these measurements. Phase-noise data characterizing the cycle slips were measured at the “Oscilloscope” port in the figure; a comparison of a high-power phase reference signal at the right side of the dashed box with the phase-locked signal from the left. Both (approximately 100-MHz) signals are divided in frequency by a factor of 10, the output of the two dividers being square-wave signals at approximately 10 MHz. Combining these two signals in a double-balanced mixer gives a dc level that shows a triangle-wave wave dependence on the phase between the two input signals, with 5 cycles up and 5 cycles down as the differential phase varies by many cycles. We assume that cycle slips are random in direction, and so the sign inversion of the slope of the triangular mixer output every 5 cycles should not impact the measured noise values. However, there is a small (≈ 5 percent) correction that must be applied due to missed phase jumps at the turnaround points of this waveform.

⁵ Charles Greenhall, personal communication, Jet Propulsion Laboratory, Pasadena, California.

⁶ See, e.g. <http://lisa.nasa.gov> or <http://lisa.esa.int>.

The PLL showed good stability at these power levels, showing no loss of lock over a period of hours unless the loop was perturbed. In order to achieve this stability, it was necessary to include a slow loop included as a part of the “PLL” in Figure 1. This slow loop adjusts a piezoelectric mirror position control in the laser and has a very wide tuning range (> 1 GHz), and acts to keep the burden on the “fast” (≈ 30 kHz) loop to a very small value.

In Figure 6, we show a comparison between laboratory measurements at 300 fW optical power and the results of simulations as the loop gain is varied. While an increase in phase slips with increasing gain may seem counterintuitive, these plots are qualitatively similar to the results of Viterbi — with the onset of phase slips occurring as the integrated phase noise within the loop bandwidth becomes greater than 1 rad^2 . The simulations were chosen to match the observed unity gain frequency of 29 kHz at the lowest gain values (8 dB attenuation). A comparison of the data with the simulation calculation shows excellent agreement for the onset of phase slips, both occurring at the “4-dB” attenuation level, and with nearly identical values.

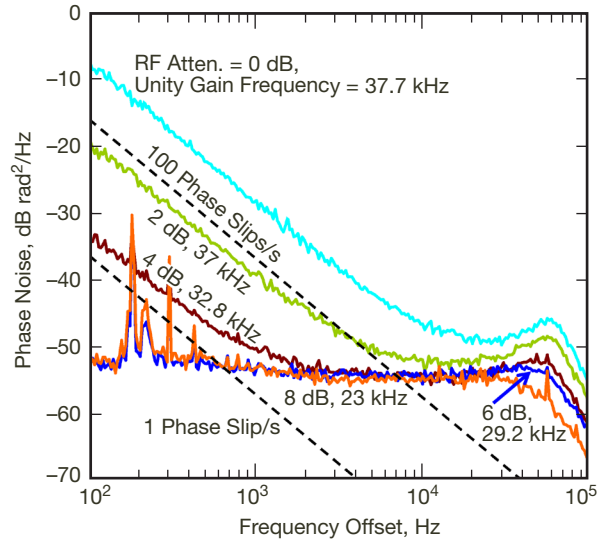
As the RF attenuation is reduced and the loop gain increased by this same factor, the observed unity gain frequency in the simulations scales roughly with this gain value, while for our measurements the unity gain frequency saturates at a value of about 38 kHz, with the data also showing increasing cycle-slip rates, compared to the simulation. We believe this discrepancy is due to the unmodeled RIN peak that can be seen at about 75 kHz for the higher gain values in Figure 6(a). These peaks showed strongly in the RF spectrum at higher gains, and gave rise to significant carrier reduction in the RF spectrum for the high gain values.

We expect that the utility of this technology will be at cycle-slip rates of 1 per second or lower where the impact of the RIN is small. This being so, the loop performance is practically equal to the theoretical prediction. Thus, while PLL performance is certainly limited by the $1/f^3$ laser phase noise, it is not practically impacted by the presence of laser RIN.

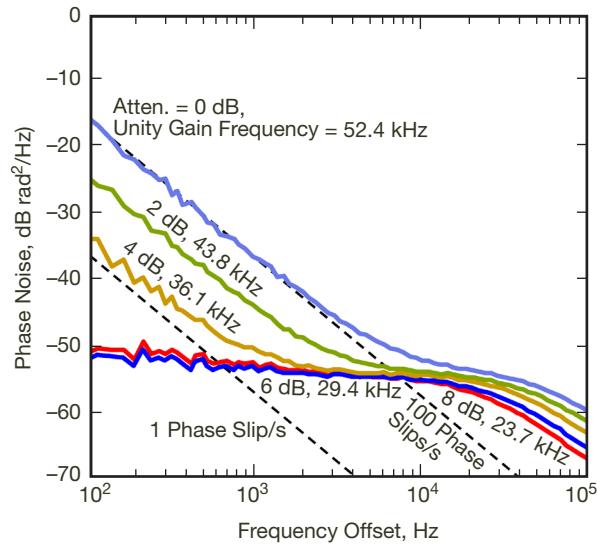
VII. Optical Ranging Performance — Use of RF Subcarriers

Figures 7 and 8 show, respectively, the block diagram and spectrum for an optical transponder scheme that includes both a pseudorandom range code (PRRC) at a relatively low rate and a 100-MHz subcarrier. In this scheme, the long-distance range ambiguity and the 100-MHz cycle ambiguity are resolved by the PRRC; the range ambiguity by use of a long code, and the cycle ambiguity by means of a relatively fast code rate and by the signal to noise in the “range code” signal. With the same signal-to-noise level, the 100-MHz signal can resolve a distance approximately 300 times smaller, so that with 30 fW of power assigned to each of these signals, a distance of 0.5 mm could be resolved at a wavelength of 1550 nm in 60 s of averaging time.

This improvement of performance can be extended to the use of higher frequency subcarriers, if the technology can be managed. Such a scheme, combining PRRC with both 100-MHz and 10-GHz subcarriers could resolve a distance of 5 microns in a time 60 s with



(a)



(b)

Figure 6. (a) Measured phase noise in the optical PLL, showing the onset of cycle slips with varying loop gain for an optical power of 300 fW into the detector. (b) Simulation calculation of PLL cycle slip phase noise due to shot noise at -55.5 dB (rad^2/Hz) for loop gains (and unity gain frequencies) comparable to the experimental tests. Lines for several phase slip rates are indicated for each graph.

detector performance equivalent to the one used in our study (5 dB worse than theoretical), and with a total power of only 100 fW (with 40 fW allocated to achieving optical phase lock).

However, in our application, the achievable tracking phase stability will be limited by performance of the frequency standard that provides a phase reference at the return of the transponded signal, possibly many minutes later. Optical frequency standards are rapidly achieving superior performance, and for such a standard with stability of $\sigma_y(1000 \text{ s}) = 1 \times 10^{-16}$, ranging accuracy would be limited to 30 microns by the optical standard perfor-

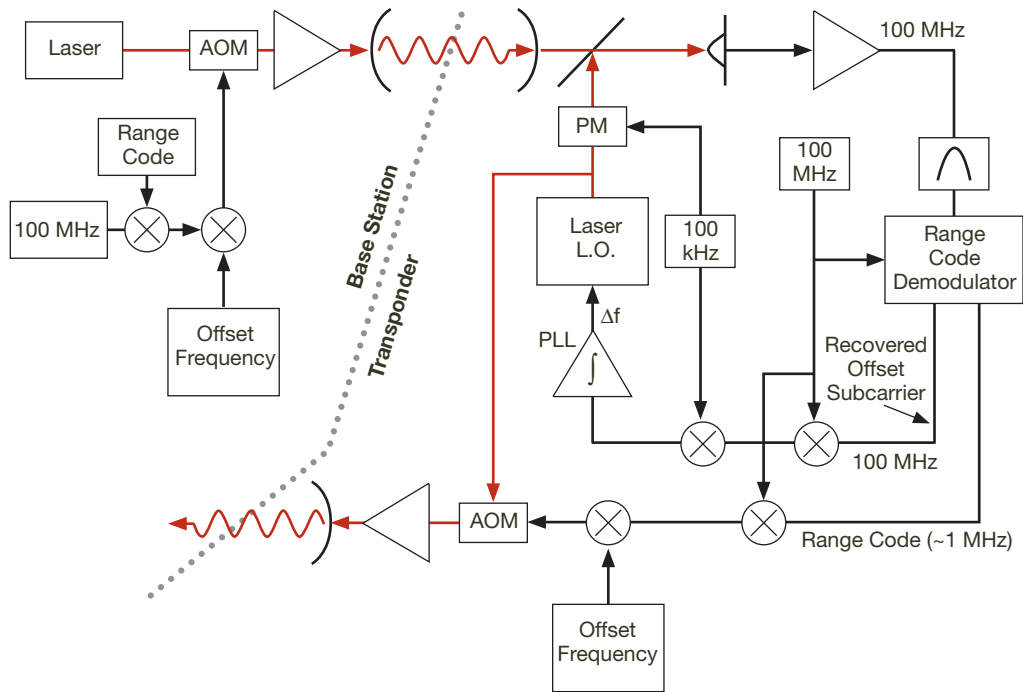


Figure 7. Block diagram for an optical base station and PLL transponder setup where a low-rate range code is applied to a 100-MHz subcarrier that is then applied to the optical signal. Optical phase lock is achieved as in the previous setup. An advantage of the subcarrier scheme is that the distance resolution is roughly the same as a 200-MHz direct range-code setup but the narrow-band signals can be kept in a “sweet spot” where the detector achieves shot-noise-limited performance.

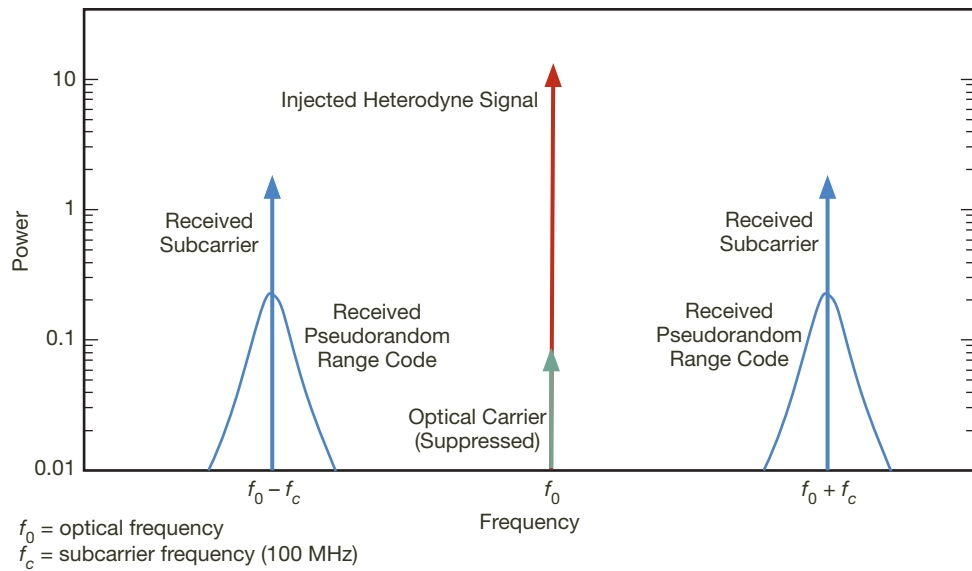


Figure 8. Spectrum for an optical carrier with the pseudorandom range code applied to a 100-MHz subcarrier.

mance, irrespective of averaging time. It is not out of reason that actual optical standard performance may be significantly better than this value, and so may very well allow better than 10-micron accuracy for a Mars mission.

VIII. Free-Space Demonstration Experiments

In addition to the PLL performance investigation, we have also performed several demonstration experiments that are designed to show that high performance can be obtained with the kind of time-varying range that a deep-space transponder would face. Of course, we can't achieve space velocities in the laboratory, but we can achieve accelerations comparable to those experienced by spacecraft, and it is these higher-order variations of phase that place a significant burden on the optical PLL circuit.

Figure 9 shows the setup for a free-space demonstration experiment that used an air track together with a corner-cube optical mirror to give excellent and stable optical performance

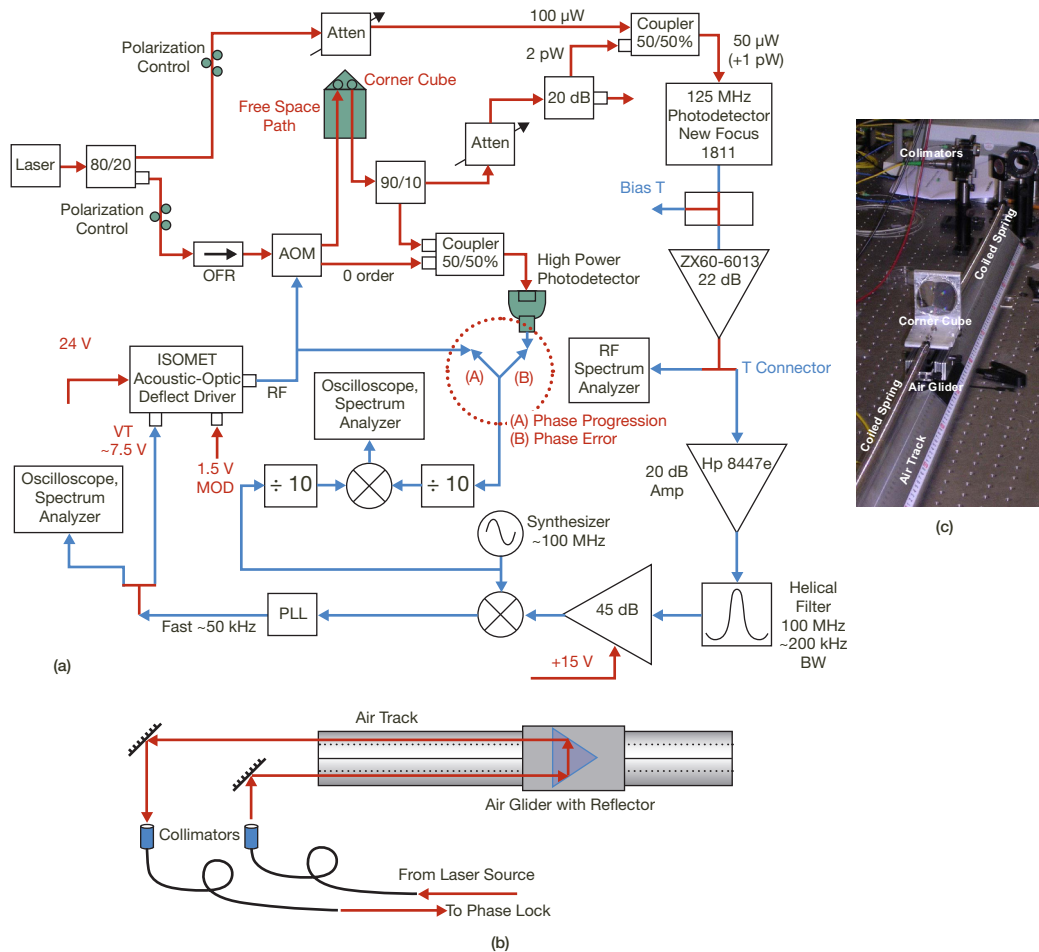


Figure 9. Details of the setup for free-space measurements using a moveable corner-cube reflector on an air track. (a) Block diagram of the electro-optical setup; (b) block diagram of the corner-cube setup; (c) photo of the corner-cube setup.

together with large mechanical motion. The corner-cube reflector was found to be necessary in order to obtain good optical performance. Coiled springs allowed accelerations up to 0.3 g to be obtained. This setup succeeded in transferring 30 percent of the optical power from the source fiber to the output fiber, with a typical variation of 5 percent due to motion of the reflector.

In initial tests at 1 pW input power, the PLL transponder showed no evidence of cycle slips when tested with free-space input from a movable corner-cube reflector mounted on an air track with springs for a period of ≈ 1 Hz and path variation of ≈ 1 m; conditions that simulate the acceleration (and associated Doppler rate) for typical orbits. These experiments were done without the use of predicts or feedforward that would be available in actual use. In these tests, the PLL phase variation was less than 0.8 rad with mirror motion of 4×10^6 rad.

A second demonstration experiment measured Doppler and Doppler errors at very low optical power (150 fW) using the moving mirror and air track, but without the springs. For this experiment, the mirror moved in a relatively smooth manner, bouncing from short springs at the ends. Figure 10 shows the setup for this experiment.

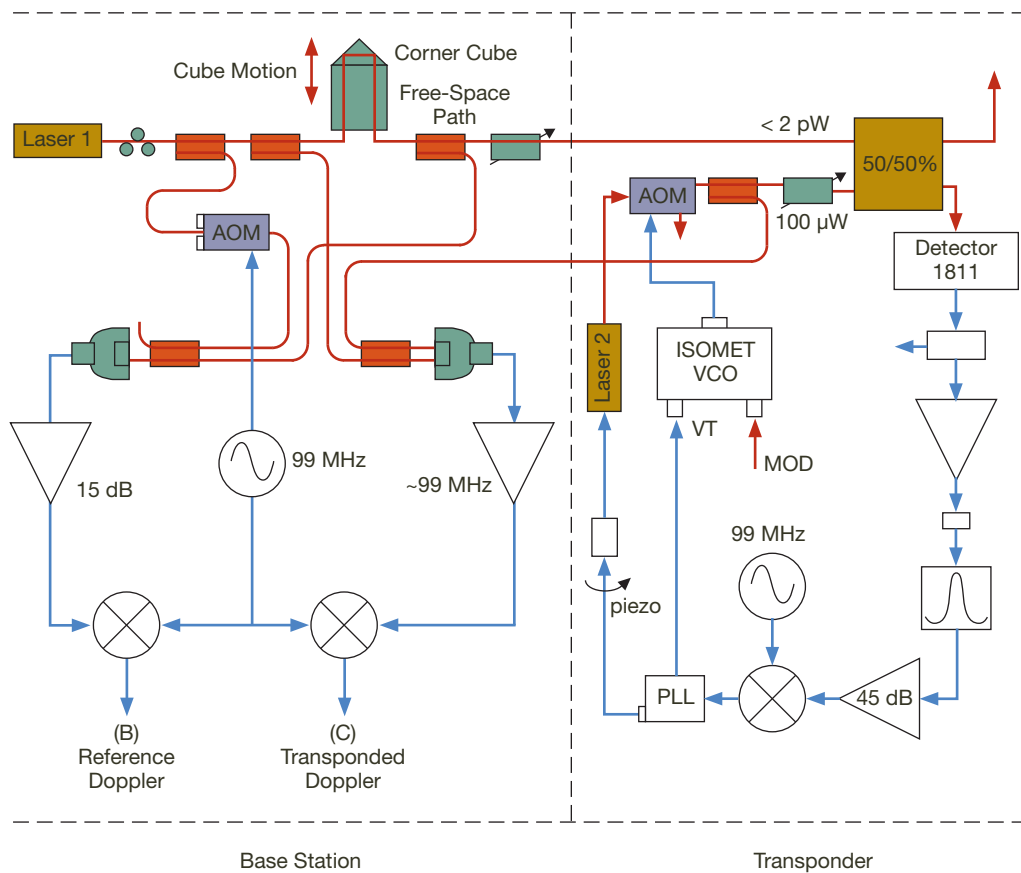


Figure 10. Block diagram for the setup used to measure Doppler and Doppler rate capability of the optical PLL at sub-pW power levels with the free-space moveable mirror.

High- and low-power Doppler measurements were obtained by simultaneously arming two counters. The raw data for both counters, showing the variation in Doppler frequency as the mirror traversed the air track for ≈ 7 out and back trips, is shown in Figure 11. A slight tilt to the track gave rise to the periodic velocity variation shown in the figure. A slight variation can be seen between the two channels at the ends where the velocity reversed.

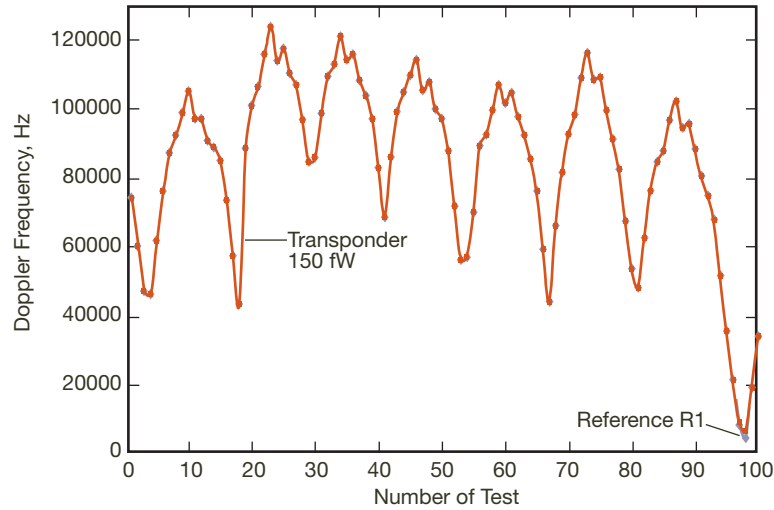


Figure 11. Low- and high-power measurements of the Doppler signal from approximately seven end-to-end mirror-motion cycles in the air-glider setup described in Figure 10 with a (low) optical power level of 150 fW. The two-way Doppler frequency offsets of 50 to 100 kHz correspond to air glider velocities of 4 to 8 cm/s, and the two curves cannot be distinguished at this resolution except at some of the bounces. The measurements consisted of simultaneous 1-s frequency measurements, taken every 2 s.

(Since it is simply measured on a counter, the Doppler signal does not show a sign reversal.)

Figure 12 shows the difference between the high- and low-power Doppler signals, showing an RMS variation of 0.2 Hz for the 1-s measurements. This corresponds to an optical

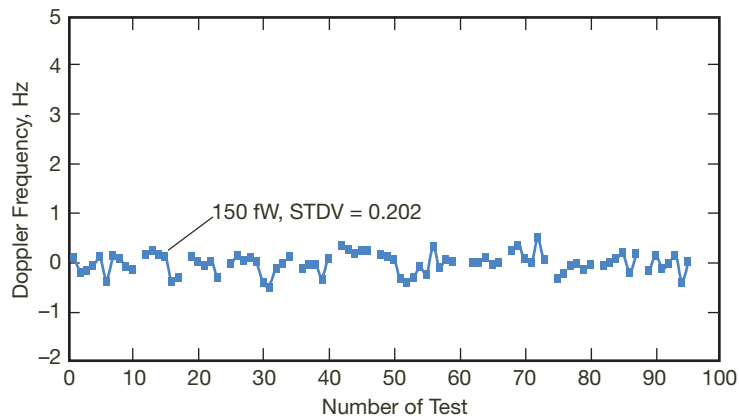


Figure 12. High-resolution data for the difference between the two curves in Figure 11. While there was no apparent phase loss between the high- and low-power signals, the HP counters gave irreproducible results for the bounces, and so these points were eliminated from the data set. The RMS variation of the points is approximately 0.2 cycles, which, for an optical frequency of 2×10^{14} Hz, corresponds to an optical frequency stability of approximately 1×10^{-15} .

frequency variation of about $\sigma_y(1\text{ s}) \approx 1 \times 10^{-15}$, a value roughly comparable to the short-term frequency stability of the best optical frequency standards today.

IX. Conclusions

A new capability for optical phase locking at ultralow optical power levels has been developed in response to an opportunity for performance improvement in deep-space ranging by the use of a coherent optical transponder. Optical phase-lock loops have been demonstrated for the first time at fW power levels. The new performance was enabled by development of a calculational methodology that simulated phase-lock operation in the presence of realistic noise models for the laser, so that optimal loop parameters could be ascertained. Low cycle-slip rates have been demonstrated at power levels as low as 40 fW, and observed cycle-slip rates were found to be in good agreement with calculated values.

The optical PLL transponder methodology seems well suited to use of standard pseudorandom range code and RF subcarrier methodologies, promising submillimeter and micron-level ranging accuracies for subcarriers at 100 MHz and 10 GHz, respectively.

Several demonstration experiments were performed using an air-track glider and a corner-cube optical reflector with approximately 1 m of free movement. Low-power phase lock was preserved with up to 0.3 g acceleration of the moving mirror, and Doppler accuracy of 0.2 cycles was demonstrated, corresponding to a stability for optical Doppler frequency measurements of $\approx 1 \times 10^{-15}$.

Acknowledgment

The authors would like to thank Ertan Salik for helpful discussions.

References

- [1] A. J. Viterbi, "Phase-Locked-Loop Behavior in the Presence of Noise," *Principles of Coherent Communication*, pp. 77–120, McGraw-Hill, 1966.
- [2] P. W. Kinman and R. M. Gagliardi, "Doppler and Range Determination for Deep Space Vehicles Using Active Optical Transponders," *Applied Optics*, vol. 27, pp. 4487–4493, November 1, 1988.
- [3] W.-T. Ni, "ASTROD (Astrodynamical Space Test of Relativity using Optical Devices) and ASTROD I," *Nucl. Phys. B (Proc. Suppl.)*, vol. 166, pp. 153–158, April 2007.
- [4] A.-C. Liao, W.-T. Ni, and J.-T. Shy, "Pico-Watt and Femto-Watt Weak-Light Phase Locking," *Int. J. Mod. Phys. D*, vol. 11, pp. 1075–1085, 2002.

- [5] W.-T. Ni, "Picowatt and Femtowatt Weak-Light Phase Locking, and its Application to Deep Space Laser Ranging," presented at 6th Edoardo Amaldi Conference on Gravitational Waves, Bankoku Shinryoukan, Okinawa, Japan, June 20–24, 2005.
http://tamago.mtk.nao.ac.jp/amaldi6/11.poster/P062_Amaldi6-weak-light-Poster.ppt
- [6] P. W. McNamara, "Weak-Light Phase Locking for LISA," *Class. Quantum Grav.*, vol. 22, issue 10, pp. S243–S247, May 2005.